

## Percolation View of Novolak Dissolution. 7. The Effect of Salts

Myoung Soo Kim and Arnost Reiser\*

Institute of Imaging Sciences, Polytechnic University, Brooklyn, New York 11201

Received January 22, 1997; Revised Manuscript Received April 25, 1997<sup>®</sup>

**ABSTRACT:** The increase in dissolution rate brought about by the addition of salt to alkaline developers is caused by the difference in the diffusivities of the OH<sup>-</sup> ions of the base and the anions of the salt. Adding salt increases the flux of cations into the film, allowing the flux of anions to increase too. The faster OH<sup>-</sup> ions, which alone control the dissolution of the resin film, benefit more from this opportunity than the salt anions. The base ions appear to diffuse about 5–10 times faster than the other anions, which suggests that OH<sup>-</sup> ions do not migrate by free volume diffusion but rather by a Grotthuss-type proton transfer mechanism. The retardation-of-dissolution effects that set in at high salt concentrations can be understood in terms of a competition of ions for the available percolation sites.

## Introduction

Since the early work of Hinsberg and Gutierrez,<sup>1</sup> it has been known that the addition of salt to an alkaline developer can strongly affect the dissolution rate of novolak films. Huang has taken up this theme in her dissertation,<sup>2</sup> where she has looked at the effect of NaCl on the dissolution rate of a novolak resin in NaOH solutions. Yamaguchi et al.<sup>3</sup> have described the effect of salt on tetramethylammonium developers. Recently, Henderson et al.<sup>4</sup> have presented an extensive investigation of the effect of salts that have a common cation with the developer base. Their study encompasses a broad range of bases and extends over a wide concentration range. Figure 1 shows some of the essential results of their work: Up to a salt concentration of about 0.7 to 0.8 M the dissolution rate increases, but at a higher salt concentration a powerful retardation effect sets in which lowers the dissolution rate. The pioneering work of Willson's group at the University of Texas at Austin has established the main facts; here, we are trying to interpret the salt effect in terms of a percolation model of novolak dissolution.

## Acceleration of Novolak Dissolution by Salts

Arcus has shown<sup>5</sup> that when a novolak film is immersed in aqueous base, a thin "penetration zone" is formed at the interface of the film with the base solution. This zone has the character of a control membrane which regulates the diffusion of base into the solid matrix. In the context of this investigation it is important to remember that the diffusional behavior of base in the penetration zone is subject to the requirement of electroneutrality: the fluxes of cations and anions must be equal.

$$F^+ = F^- \quad (1)$$

For example, if a novolak film is dissolving in a solution of pure KOH, the ionic fluxes into the matrix are<sup>2,6</sup>

$$\begin{aligned} F^+ &= \text{grad}[K^+]D_{K^+} \\ F^- &= \text{grad}[OH^-]D'_{OH^-} \end{aligned} \quad (2)$$

Square brackets denote molar concentrations,  $D_{K^+}$  is the (mean) diffusion coefficient of potassium ions in the penetration zone,  $D'_{OH^-}$  is the effective diffusion coefficient of hydroxyl ions.

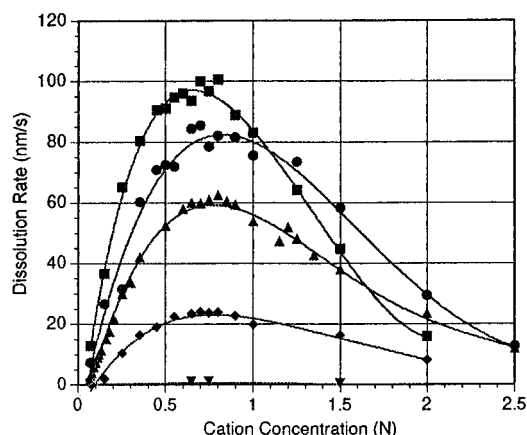


**Figure 1.** Effect of cation type and salt concentration on dissolution rate. Base concentration: 0.07 N. Reprinted with permission from ref 4. Copyright 1996 SPIE.

In order to keep the following derivation simple we shall assume that the diffusion coefficients of the ions and the concentration gradients are constant across the zone. Such an assumption is by no means correct,<sup>7</sup> and we shall have to take account of this at a later stage. For the time being, using the above assumption, we may apply Fick's law in its simplest form and express the ionic fluxes as proportional to the ionic concentrations in the developer.

$$\begin{aligned} F^+ &= \text{const} \times [K^+]D_{K^+} = \text{const} \times [KOH]D_{K^+} \\ F^- &= \text{const} \times [OH^-]D'_{OH^-} = \text{const} \times [KOH]D'_{OH^-} \end{aligned} \quad (3)$$

Equating the cation flux with the anion flux one finds

$$D'_{OH^-} = D_{K^+}$$

which means that, in a film dissolving in a developer of pure KOH, the OH<sup>-</sup> ions diffuse with the migration rate of the cations.

When a salt, e.g. KCl, is added to the developer, the cationic flux into the matrix increases, and that allows the anionic flux to increase too. The anionic flux has now two components, and those make different contributions to the flux of negative charge. Assuming that these contributions are proportional to the diffusion coefficients of the anions, the anionic flux may be expressed in the following form:

$$F^- = [KOH]D'_{OH^-} + [KCl]D'_{Cl^-} \quad (4)$$

<sup>®</sup> Abstract published in *Advance ACS Abstracts*, June 15, 1997.

The dissolution rate of novolak is controlled by the diffusion of  $\text{OH}^-$  ions. If we observe an increase in the dissolution rate, this means that the flux of  $\text{OH}^-$  ions into the matrix has increased. Such an increase is possible only if the effective diffusion coefficient of  $\text{OH}^-$  ions in these systems is significantly larger than that of  $\text{Cl}^-$  ions. The difference in diffusivity between  $\text{OH}^-$  and other anions is ultimately the cause of the acceleration effect.

In general, the salt effect depends on both the base concentration and the concentration of the added salt; here, we shall deal only with the behavior of systems at a fixed base concentration. We have chosen as our standard condition a base concentration of 0.10 N, which is quite near to the experimental conditions used by Willson's group at Austin.

In establishing a relation between the dissolution rate and the composition of the developer, we introduce the concentration ratio of salt and base

$$\frac{[\text{KCl}]}{[\text{KOH}]} = y \quad (5)$$

and the ratio of the effective diffusion coefficients of the two anionic components.

$$\frac{D_{\text{Cl}^-}}{D_{\text{OH}^-}} = \alpha \quad (6)$$

The electroneutrality condition (eq 1) can now be expressed in terms of  $y$

$$D_{\text{OH}^-} = (1 + y)D_{\text{K}^+} - yD_{\text{Cl}^-} \quad (7)$$

With  $D_{\text{Cl}^-}$  eliminated via eq 6, this can be written in the form

$$D_{\text{OH}^-} = \frac{1 + y}{1 + \alpha y} D_{\text{K}^+} \quad (8)$$

We have plotted the acceleration function  $Y$

$$Y = \frac{1 + y}{1 + \alpha y} \quad (9)$$

in Figure 2, where it can be seen that, for  $y$  going to infinity, the acceleration function  $Y$  tends to the limit

$$(\lim Y)_{y \rightarrow \infty} = \frac{1/y + 1}{1/y + \alpha} = \frac{1}{\alpha} \quad (10)$$

The value of  $\alpha$  in the acceleration function matters a great deal. For  $\alpha = 0.1$  there is a steep rise in the effective diffusion coefficient of  $\text{OH}^-$  ions as the salt concentration increases, and that means that there is an equivalent rise in dissolution rate. With  $\alpha = 0.2$ , the rise in the diffusion coefficient of base is less pronounced, and with  $\alpha = 0.5$ , it is quite modest. We conclude that the effective diffusion coefficient of  $\text{OH}^-$  ions must be significantly larger than that of  $\text{Cl}^-$  ions to produce the observed acceleration of novolak dissolution.

In terms of eq 8 the slope of a (nonlogarithmic) plot of  $D_{\text{OH}^-}$  vs  $y$  is given by

$$\left( \frac{dD_{\text{OH}^-}}{dy} \right)_{y=0} = (1 - \alpha)D_{\text{K}^+} \quad (11)$$

This slope depends on the diffusion coefficient of the cation, in qualitative agreement with the data of Henderson et al.<sup>4</sup> (Figure 1). The anion of the salt, chloride

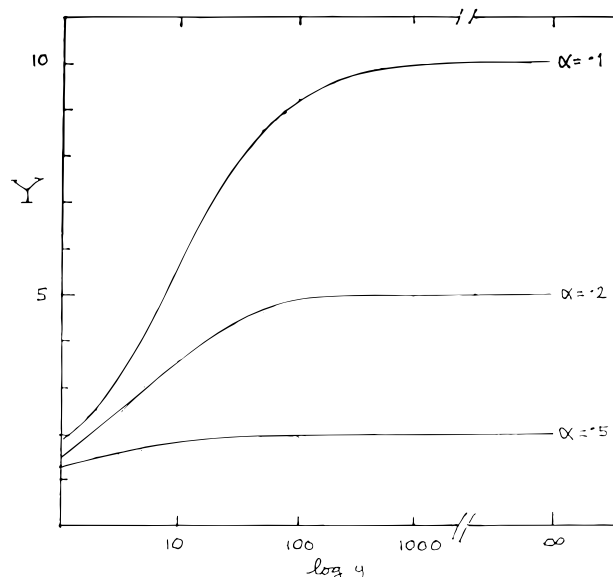


**Figure 2.** Acceleration function  $Y = (1 + y)/(1 + \alpha y)$ .  $y = [\text{salt}]/[\text{base}]$  is the dimensionless salt concentration.

in Figure 1 of the Henderson paper, affects the slope via the factor  $(1 - \alpha)$ .

### Retardation of Novolak Dissolution

Fick's law coupled with the requirement of electro-neutrality explains the increase in dissolution rate brought about by salt, but it cannot explain the downward branch of the Henderson–Willson curves. For the diffusivity function to decrease, a genuine lowering of the flux of  $\text{OH}^-$  ions must occur in the system.

How can the presence of salt produce such an effect? We believe that the answer is linked to the percolative nature of the diffusion process. In a percolation system, the elementary step of base diffusion is the transfer of an  $\text{OH}^-$  ion from one hydrophilic site to the next.<sup>8,9</sup> For this step to occur, a vacant percolation site must be available in the vicinity of the diffusing particle. As more and more sites are being occupied by (slow moving)  $\text{Cl}^-$  ions, some of the hydroxyl ions will have to wait until a suitable site clears. The higher the chloride concentration is, the longer the wait. At some point the hydroxyl ions will be completely surrounded by chloride ions and will be forced to migrate with their speed. This will occur at a critical chloride ion concentration  $[\text{Cl}^-]_c$ .

We can introduce an element of competition for percolation sites into our model by assuming that in the presence of chloride ions the effective diffusion coefficient of hydroxyl ions,  $D'_{\text{OH}^-}$ , which now includes the retardation effect, is determined by the number of open sites in the percolation field, i.e. those sites that are not occupied by  $\text{Cl}^-$  ions. We assume that the fraction of sites occupied by  $\text{Cl}^-$  ions in the immediate surroundings of a base ion is the ratio

$$[\text{Cl}^-]/[\text{Cl}^-]_c$$

With this the fraction of vacant sites becomes

$$1 - [\text{Cl}^-]/[\text{Cl}^-]_c$$

The ratio  $[\text{Cl}^-]/[\text{Cl}^-]_c$  is equal to the ratio  $[\text{KCl}]/[\text{KCl}]_c$  which defines a critical value  $y_c$  of the dimensionless composition variable  $y$ .

$$[\text{KCl}]/[\text{KCl}]_c = y/y_c \quad (12)$$

At  $y = y_c$ ,  $D'_{OH^-}$  equals  $D_{Cl^-}$ .

We can now describe the salt effect of development by the following approximation: in a system which has the composition  $y$ , a fraction  $(1 - y/y_c)$  of  $OH^-$  ions will move with the diffusivity  $D'_{OH^-}$ , another fraction,  $y/y_c$ , will move with the diffusivity of chloride,  $D_{Cl^-}$ . The overall transport of  $OH^-$  ions will occur with an observed effective diffusion coefficient  $D'_{OH^-}$ , which now takes account of the retardation effect.

$$D'_{OH^-} = (1 - y/y_c)D'_{OH^-} + y/y_c D_{Cl^-} \quad (13)$$

Eliminating  $D_{Cl^-}$  via  $\alpha$ , eq 13 can be written in the form

$$D'_{OH^-} = D'_{OH^-} \{1 - (1 - \alpha)y/y_c\} = D'_{OH^-} G \quad (14)$$

where  $G$  is the retardation function

$$G(y, y_c, \alpha) = 1 - (1 - \alpha)y/y_c \quad (15)$$

### The Base Diffusivity Function $D_{OH^-}(y)$

The observed diffusion coefficient,  $D'_{OH^-}$ , of eq 14 describes the dissolution behavior of the system over the whole range of the variable  $y$ . It may be termed the base diffusivity function, and we shall denote it in the following by  $D_{OH^-}$ . The diffusivity function is the product of three factors: the diffusivity of the cations, the acceleration function  $Y$  and the retardation function  $G$ .

$$D_{OH^-} = D_{K^+} YG = D_{K^+} \frac{1+y}{1+\alpha y} \left\{ 1 - (1 - \alpha) \frac{y}{y_c} \right\} \quad (16)$$

Equation 16 replaces and supersedes eq 8.

We can now determine some of the properties of the diffusivity function. To find the maximum of the function we differentiate it with respect to  $y$  and put the derivative equal to zero.

$$dD_{OH^-}/dy = D_{K^+} \{ Y(dG/dy) + G(dY/dy) \} = 0 \quad (17)$$

where

$$dY/dy = (1 - \alpha)/(1 + \alpha y)^2 \quad (18)$$

$$dG/dy = -(1 - \alpha)/y_c \quad (19)$$

From this the position of the maximum ( $y_m$ ) is found in the form

$$y_m = z_{1,2} y_c = \{-1 + [1 + \alpha y_c]^{1/2}\} / \alpha \quad (20)$$

The position of the maximum of diffusivity is independent of  $D_{K^+}$ , in agreement with the experimental data of Henderson et al.<sup>4</sup> The base diffusivity at the maximum is obtained by inserting  $y_m$  into eq 16. The slope of the diffusivity curve is given by the general expression

$$dD_{OH^-}/dy = D_{K^+} \{ Y(dG/dy) + G(dY/dy) \} \quad (21)$$

and the initial slope at  $y = 0$  is

$$\{dD_{OH^-}/dy\}_{y=0} = D_{K^+} (1 - \alpha)(1 - 1/y_c) \quad (22)$$

which replaces and supersedes eq 11.

### Nonlinear Relation between $OH^-$ Flux and Base Concentration

We mentioned at the outset that the diffusion model presented above assumes (eq 3) that the concentration

gradient of ions in the penetration zone is directly proportional to their concentration in the developer. In particular, the gradient of  $OH^-$  ions is proportional to the base concentration ( $c_B$ ).

$$\text{grad}[OH^-] = (1/\delta)c_B \quad (23)$$

This implies also that the flux of  $OH^-$  ions through the penetration zone is a linear function of  $c_B$ . In reality, this function is far from linear;<sup>7</sup> and that is reflected in the well-known supralinear dependence of the dissolution rate on base concentration, as illustrated in Figure 3a. In that figure we have plotted the dissolution rate of a typical novolak resin as a function of the normality of KOH.

The cause of the nonlinear behavior of the dissolution rate is the profile of the base concentration in the penetration zone. (Figure 4). The interface of the zone with the virgin matrix is a fractal surface<sup>10</sup> which produces a concentration gradient at the front of the zone. This gradient depends on the base concentration and it is considerably steeper than the ratio  $c_B/\delta$ . In applying our diffusion model to the experimental results, the nonlinearity of the diffusion coefficient must be taken into account. The data in Figure 3 provide a means of doing so. It can be seen in Figure 3a that dissolution sets in at a threshold base concentration,  $c_B^0$ . Furthermore, the experimentally observed dissolution rate,  $R_{\text{exp}}$ , is a quadratic function of the difference ( $c_B - c_B^0$ ). (Figure 3b).

$$R_{\text{exp}} = k_1 (c_B - c_B^0)^2 \quad (24)$$

In the absence of this nonlinearity the relation between  $R$  and  $(c_B - c_B^0)$  would be represented by the straight line in the lower part of Figure 3a.

$$R_{\text{lin}} = k_2 (c_B - c_B^0) \quad (25)$$

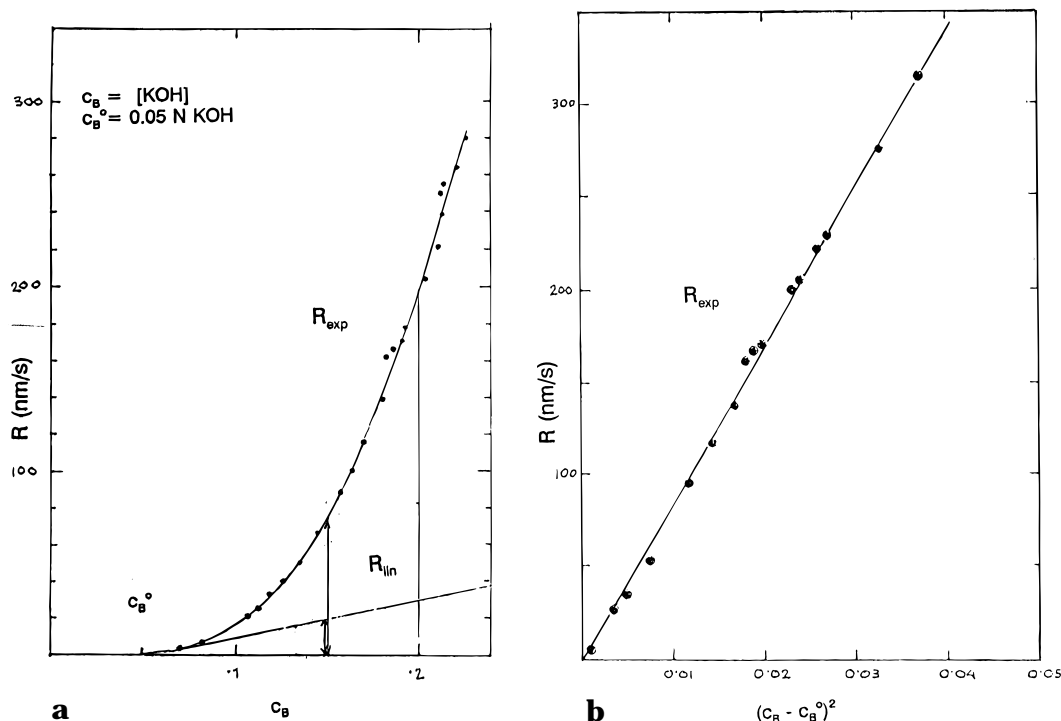
The transformation of the experimental values of dissolution rate,  $R_{\text{exp}}$ , into the corresponding linearized values,  $R_{\text{lin}}$ , is achieved by eq 26.

$$R_{\text{lin}} = \sqrt{(k_2^2/k_1)} \sqrt{R_{\text{exp}}} \quad (26)$$

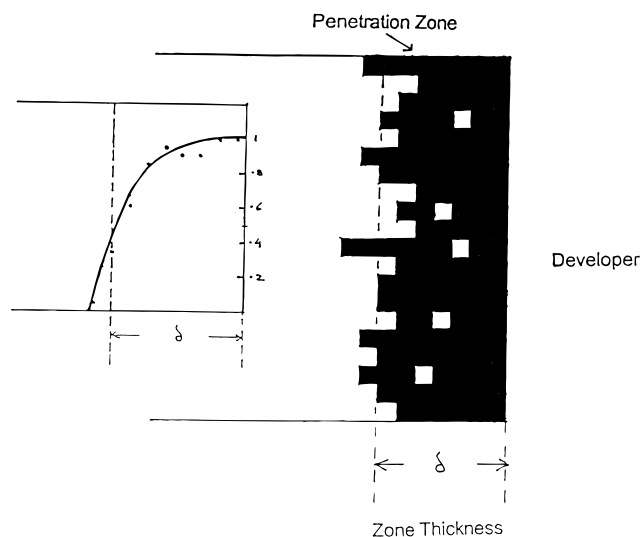
The value of  $k_1$  is obtained from the slope of the straight line in Figure 3b and that of  $k_2$  from the slope of the straight line in Figure 3a. The linearized data can now be used in eq 16. Figure 5 shows the result of the linearizing procedure applied to the experimental data for KCl in 0.1 KOH. The upper curve represents the immediate results of the experiments,  $R_{\text{exp}}/R^0_{\text{exp}}$ ; the lower curve shows the linearized data,  $R_{\text{lin}}/R^0_{\text{lin}}$ , obtained by eq 26. In both cases,  $R^0$  represents the dissolution rate in pure base.

### Extracting the Diffusional Parameters $\alpha$ and $y_c$ from the Experimental Data

The parameters  $\alpha$  and  $y_c$  are obtained by fitting eq 16 to the linearized data. We have used the SigmaPlot least-squares fitting program to do this, and have started the fitting procedure by estimating  $y_c$  as that value of  $y$  at which  $R/R^0$  is approximately 0.9. How well the data can be fitted by an iteration procedure of this kind is shown in Figure 6 where, for KCl in 0.1 N KOH, we have plotted  $\{R_{\text{exp}}/R^0_{\text{exp}}\}^{1/2} = R_{\text{lin}}/R^0_{\text{lin}}$  and compared it with the theoretical equation 16 for  $D_{OH^-}/D_{K^+}$ , using  $\alpha = 0.18$  and  $y_c = 32.3$ .

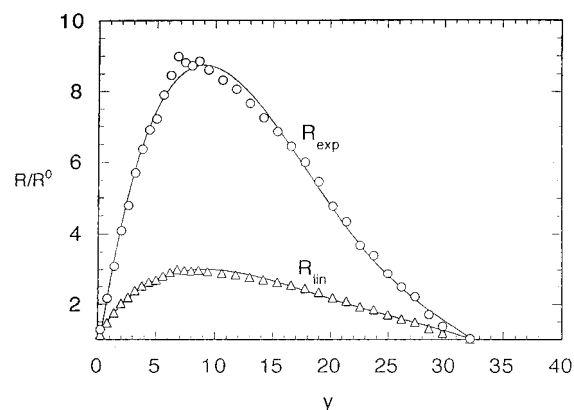


**Figure 3.** (a) Plot of the dissolution rate of a novolak film in KOH as a function of the base concentration  $c_B$  (N). Dissolution sets in at the threshold  $c_B^0$ . (b) Plot of the dissolution rate of a novolak film as a function of the square  $(c_B - c_B^0)^2$ .

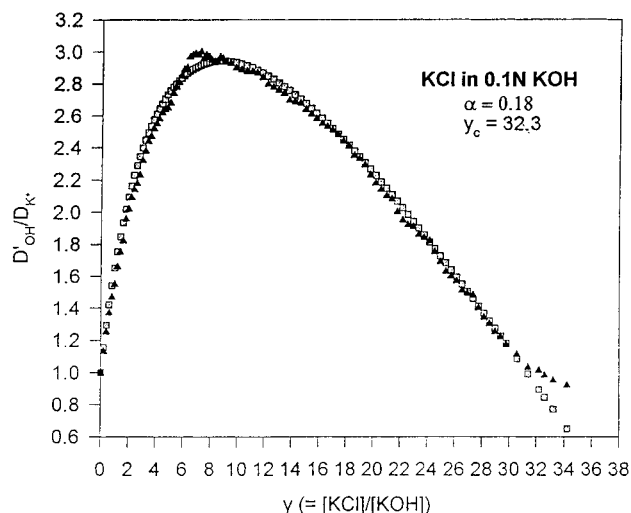


**Figure 4.** Penetration zone formed in a resin film dissolving in aqueous base. The black squares represent sites of phenolate ions; the white squares are undepronated phenolic sites.

We have investigated the mixed developers (LiOH + LiCl), (NaOH + NaCl), (KOH + KCl), (RbOH + RbCl), and (CsOH + CsCl). The diffusional parameters of these systems are collected in Table 1. Figure 7a shows the experimental data for the alkali chlorides; Figure 7b shows the linearized data and the theoretical curves. Equation 16 provides a good description of the salt effect in every case, although different values of  $\alpha$  have to be used for different cations. Table 2 lists the values of  $\alpha$  in the bases LiOH to CsOH. Since  $\alpha$  is defined as the ratio of *anionic* diffusivities, it is not expected to depend on the nature of the cation. After some puzzlement, we found that the changes in  $\alpha$  are not caused by the nature of the cation, but are the result of differences in the overall ionic flux, i.e. the dissolution rate in the different bases. We tested this by measuring  $\alpha$  in mixtures of KOH and KCl at different base concentrations ( $c_B$ ). The



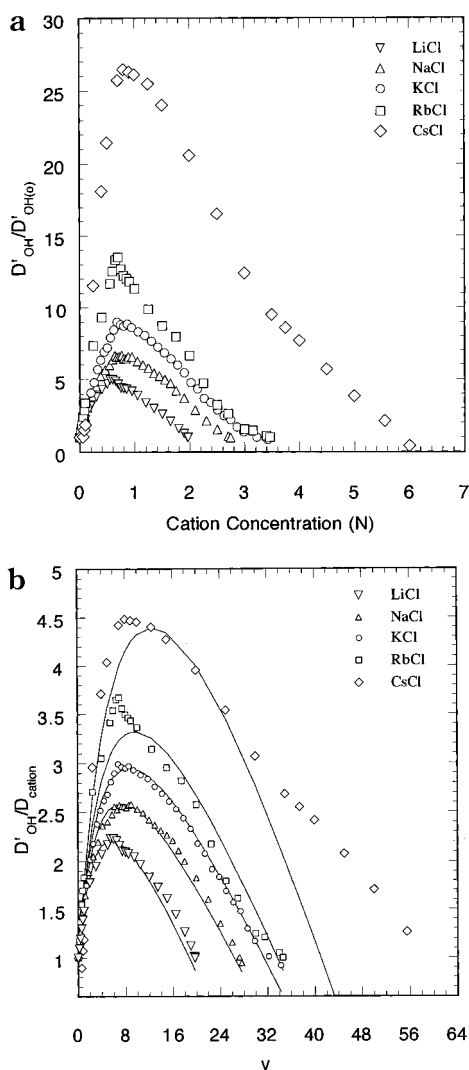
**Figure 5.** Experimental dissolution rate values and linearized values obtained through eq 26. Both are plotted as functions of the dimensionless salt concentration  $y$ .



**Figure 6.** Theoretical diffusivities function  $D_{OH^-}/D_{K^+}$  derived from eq 16 for  $\alpha = 0.18$  and  $y_c = 32.3$ , compared with the linearized values of the dissolution rate from Figure 5.

**Table 1. Listing of Characteristic Parameters for all the Salts of this Study<sup>a</sup>**

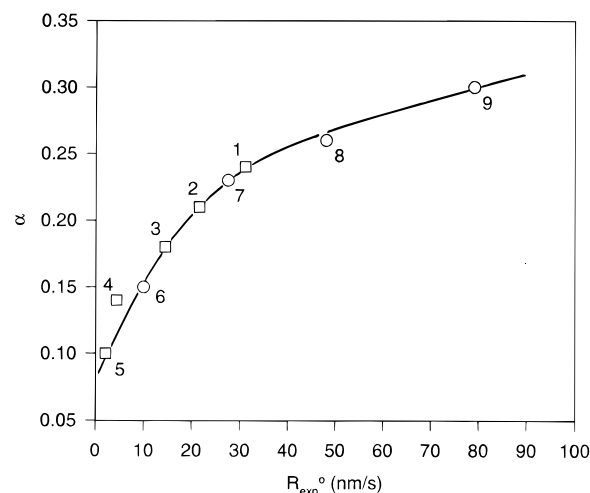
salt	$\alpha$	$y_c$	$r_i$	$(r^+ + r^-)$
1. Li <sup>+</sup> Cl <sup>-</sup>	0.24	20	0.60	2.41
2. Na <sup>+</sup>	0.21	27	0.95	2.76
3. K <sup>+</sup>	0.18	32	1.33	3.14
4. Rb <sup>+</sup>	0.14	33	1.48	3.29
5. Cs <sup>+</sup>	0.10	42	1.69	3.50
6. TMA <sup>+</sup>	0.13	55	2.70	4.50
7. K <sup>+</sup> F <sup>-</sup>	0.17	31	1.36	2.69
8. Cl <sup>-</sup>	0.18	32	1.81	3.14
9. Br <sup>-</sup>	0.18	30	1.96	3.29
10. I <sup>-</sup>	0.19	36	2.16	3.49
11. CN <sup>-</sup>	0.17	31	1.6	2.93
12. SCN <sup>-</sup>	0.20	55	3.5	4.83
13. K <sub>3</sub> -citrate	0.19	65	4.5?	5.8?
14. Na <sup>+</sup> Cl <sup>-</sup>	0.21	27	1.81	2.76
15. Na-propionate	0.19	35	2.4	3.35
16. Na <sub>2</sub> -malonate	0.25	36	2.5	3.45

<sup>a</sup> Base concentration: 0.1 N.**Figure 7.** (a) Experimental diffusivities of OH<sup>-</sup> ions in film dissolving in 0.1 N KOH. (b) Linearized diffusivities and the theoretical curves derived from eq 16.

value of  $\alpha$  depends clearly on the dissolution rate in pure base and the data points for the system (KOH + KCl) and for the bases LiOH, NaOH, KOH, and RbOH fall on the same  $\alpha$  vs  $R_{exp}$  plot. (See Figure 8.) The decrease in  $\alpha$  with the ionic flux indicates that the distinction between OH<sup>-</sup> ions and the other anions becomes more pronounced at lower ionic fluxes. The values of Table

**Table 2. Diffusivity Ratio  $\alpha = D_{Cl^-}/D_{OH^-}$  and Dissolution Rate in Pure Base**

	$R_{exp}$ (nm/s)	$\alpha$
1. LiCl + 0.1 N LiOH	31.1	0.24
2. NaCl + 0.1 N NaOH	21.5	0.21
3. KCl + 0.1 N KOH	14.4	0.18
4. RbCl + 0.1 N RbOH	4.36	0.14
5. CsCl + 0.1 N CsOH	2.07	0.10
6. KCl + 0.09 N KOH	9.95	0.15
7. KCl + 0.11 N KOH	27.5	0.23
8. KCl + 0.13 N KOH	48.1	0.26
9. KCl + 0.15 N KOH	79.1	0.30

**Figure 8.** Values of the anionic diffusivity ratios  $\alpha = (D_{X^-}/D_{OH^-})$  for the five alkali metal bases (squares), and for the system KCl + KOH at different base concentrations (circles) plotted as a function of the dissolution rate  $R_{exp}^0$  in the pure base.**Table 3. Cationic Diffusivities derived from Dissolution Rates in 0.1 N Solutions**

ion	$10^{15} D_{exp}$ (cm <sup>2</sup> /s)
Li <sup>+</sup>	31.1
Na <sup>+</sup>	21.5
K <sup>+</sup>	14.4
Rb <sup>+</sup>	4.4
Cs <sup>+</sup>	2.1

2 extrapolated to a dissolution rate of zero give a limiting value of  $\alpha = 0.10$ , which may be regarded as the ratio of ionic mobilities in the absence of a concentration gradient. The dependence of ionic diffusivities, and of the ratio  $\alpha$ , on the base concentration in the developer and hence on ionic flux in the penetration zone is not well understood. We are planning a more detailed study of this aspect for the near future.

### Mechanism of Base Diffusion in the Penetration Zone

Diffusion coefficients of cations can be obtained from dissolution rates by multiplication with the thickness ( $\delta$ ) of the penetration zone.

$$D = R\delta \quad (27)$$

In the absence of more specific information, following Arcus,<sup>5</sup> we have assumed throughout a zone thickness of  $\delta = 100$  Å. Cationic diffusion coefficients for 0.1 N KOH based on this assumption are listed in Table 3.

Anionic diffusivities are not accessible in this way, and all we can determine from our experiments are the ratios,  $\alpha$ , of anionic diffusivities. The values of  $\alpha$  derived

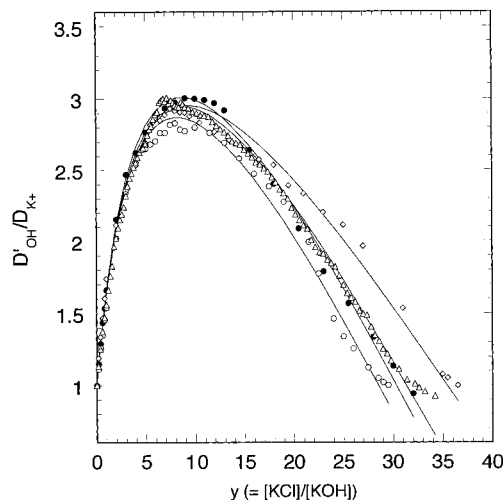
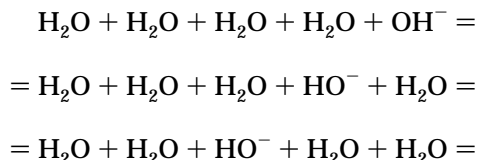
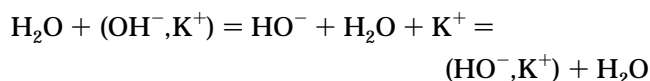


**Figure 9.** Salt effect curves for the potassium halogenides (0.1 N base).

for the salt effect of the potassium halogenides in standard 0.1 N KOH, shown in Figure 9, are all in the vicinity of  $\alpha = 0.2$ . That is an important result: it means that in the penetration zone the  $\text{OH}^-$  ions travel at least 5 times faster than any other anions. Since the  $\text{OH}^-$  ions are comparable in size with the others (the crystallographic radius of  $\text{OH}^-$  is 1.37 Å and that of  $\text{F}^-$  is 1.33 Å),<sup>11</sup> this suggests that  $\text{OH}^-$  ions migrate through the penetration zone by a mechanism different from simple free volume diffusion. We believe that in the penetration zone the base function propagates through a sequence of proton transfer steps,<sup>12,13</sup> a mechanism that goes back to Grotthuss (1805).



We support this suggestion by describing the genesis of the penetration zone in more detail. Whenever a base (hydroxyl) anion enters the novolak film and encounters a phenol group, it deprotonates it to a phenolate ion. In this process the base ion disappears and is replaced by a molecule of water. The base anions travel with their counteranions, and as a result, after the deprotonation step, a group of three particles finds itself at the location of the former phenol group: the polymer-bound phenolate ion, its counteranion, and a molecule of water. When the next base ion-pair (e.g.,  $\text{K}^+\text{OH}^-$ ) enters the matrix, it will react with the water at the location of the phenolate site



and will become associated with the site which will now be constituted of five particles: the phenolate ion, its counteranion, the base ion-pair and a molecule of water. As more base enters the matrix, the penetration zone grows and may be described as an ensemble of such sites. Incoming base then travels through the zone by a series of proton transfer steps within the water chain associated with the continuous line of phenolate sites, in analogy with the scheme of the Grotthuss mechanism indicated above.

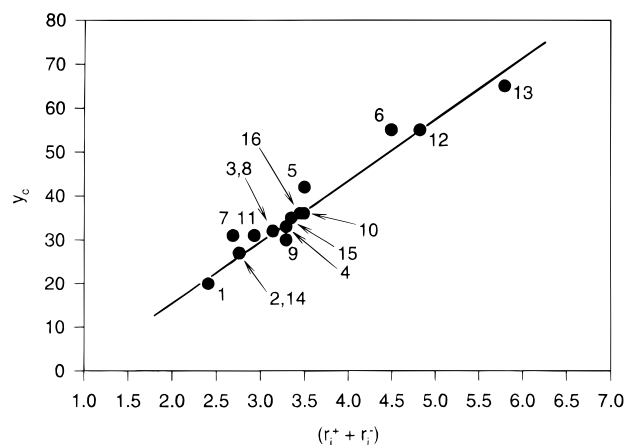


**Figure 10.** Values of  $y_c$  of the salts listed in Table 1 plotted against the sum of the cationic and the anionic radii.

If this view is correct, it may fundamentally alter our understanding of the dissolution mechanism. Base diffusion across the zone need not be the rate-determining process, the rate-controlling event may be the deprotonation step at the frontal interface of the zone with the virgin matrix. Certainty about this point is important for an understanding of, e.g., the large effect of resin molecular weight on dissolution rate. A crucial experiment, either confirming the Grotthuss mechanism of base diffusion or disproving it, would be highly desirable.

**Acknowledgment.** We are grateful to the Semiconductor Research Corporation, and to Hoechst Celanese Corporation for financial support of this work. We have greatly benefited from discussions with Grant Willson and his group at the University of Texas, Austin, in particular Dr. Clifford Henderson and Pavlos Tsiartas.

## Appendix

**Meaning of the Critical Composition  $y_c$ .** The parameter  $y_c$  represents that number of  $\text{X}^-$  anions which (statistically) surround every base anion ( $\text{OH}^-$ ) at the point where the base ions are forced to migrate with the diffusion rate of the  $\text{X}^-$  ions. In a simple cubic lattice the number of sites surrounding a central ion is 26. If both types of ions bind equally to the percolation sites, 26  $\text{X}^-$  ions surrounding every base ion completely impede the independent progress of base. If the  $\text{X}^-$  ions are bound less strongly than the base ions to the percolation sites, a larger number of  $\text{X}^-$  ions will be needed to do this, and  $y_c$  will be larger than 26. If  $\text{X}^-$  is bound more strongly,  $y_c$  will be smaller. It is the relative bonding strength of the two types of ions which affects the statistics of competition.

What determines ion bonding in the penetration zone? The stationary, polymer-bound phenolate ions of the penetration zone are occupied in the first place by their associated counteranions, and so both anions ( $\text{OH}^-$  and  $\text{X}^-$ ) are bonding onto these counter cations. The energy of bonding depends on the surface potentials,  $V$ , of the ions (eq 28), and since both the counter cations and the anions are involved in bonding to the percolation sites, a linear relation between  $y_c$  and the sum of the cationic and anionic radii of the salts is expected.

$$V = \text{const} \times \frac{1}{r^+ + r^-} \quad (28)$$

Figure 10 shows that there is a convincing correlation between  $y_c$  and the sum of the ionic sizes of the paired

ions. (The numbers in Figure 10 correspond to the data in Table 1). We believe that this supports the idea of the retardation effect being caused by the competition of ions for the available percolation sites.

### References and Notes

- (1) Hinsberg, W. D.; Gutierrez, M. L. *Proc. SPIE* **1984**, 469, 57.
- (2) Huang, J. P. Dissertation, Polytechnic University, Brooklyn, NY, May 1989, pp 83–88.
- (3) Yamaguchi, A.; Kishimura, S.; Yamada, Y.; Nagata, H. *Jpn. J. Appl. Phys.* **1991**, 30, 195.
- (4) Henderson, C. L.; Tsiartas, P. C.; Clayton, K. D.; Pancholi, S.; Pawlowski, A.; Simpson, L. L.; Willson, C. G. *Proc. SPIE* **1996**, 2724, 481.
- (5) Arcus, R. A. *Proc. SPIE* **1986**, 631, 124.
- (6) Huang, J. P.; Kwei, T. K.; Reiser, A. *Macromolecules* **1989**, 223, 4106.
- (7) Yeh, T. F.; Shih, H. Y.; Reiser, A.; Toukhy, M. A.; Beauchemin, B. T. *J. Vac. Sci. Technol.* **1990**, 10 B, 715.
- (8) Yeh, T. F.; Shih, H. Y.; Reiser, A. *Macromolecules* **1992**, 25, 5345.
- (9) Stauffer, D. *Introduction to Percolation Theory*, Taylor & Francis: London 1985.
- (10) Reiser, A.; Shih, H. Y.; Yeh, T. F.; Huang, J. P. *Angew. Chem., Int. Ed. Engl.* **1996**, 35, 2428–2440.
- (11) Shannon, R. P. *Acta Crystallogr.* **1974**, A 32, 751.
- (12) Walden, F. W. Z. *Phys. Chem.* **1906**, 55, 207, 246.
- (13) Huggins, M. L. *J. Am. Chem. Soc.* **1931**, 53, 3190.

MA970081S